Linear Instability of Entry Flow in a Pipe

Kirti Chandra Sahu

Rama Govindarajan
e-mail: rama@jncasr.ac.in

Engineering Mechanics Unit,
Jawaharlal Nehru Centre for Advanced
Scientific Research,
Bangalore-560 064, India

We show that flow in the entry region of a circular pipe is linearly unstable at a Reynolds number of 1000, a factor of 10 smaller than assumed hitherto. The implication that dynamics in this region could greatly hasten the transition to turbulence assumes relevance because in spite of major recent progress, the issue of how pipe flow becomes turbulent is far from settled. Being axisymmetric and close to the centerline, the present instability would be easily distinguishable in an experiment from other generators of turbulence. [DOI: 10.1115/1.2776965]

1 Introduction

The fully developed laminar flow through a circular pipe is linearly stable at any Reynolds number (see, e.g., Ref. [1]). The mechanisms driving the flow to turbulence are being investigated avidly [2–7]. When and whether the transient algebraic growth of disturbances is crucial or whether the route is entirely nonlinear [8] is still not clear. In this paper, we do not address this debate. Our purpose is to bring to light a factor, which has hitherto been considered unimportant, namely, the exponential growth of disturbances in the entry region. Thus, the very assumption that the flow is fully developed could obscure the complete route to turbulence. The distance l_e from the pipe entrance required to reach the fully developed parabolic profile can be very long [9–11] and scales linearly with the Reynolds number Re, roughly as $l_e/R \sim \mathrm{Re}/20$, where R is the pipe radius. This means that high Reynolds number laminar flow through a pipe of limited length may never reach a parabolic state. With many recent demonstrations [2,12] that pipe flow may be maintained laminar up to very high Reynolds numbers (of the order of hundred thousand), an understanding of the instability of the entry flow is increasingly relevant. Even at much lower Reynolds numbers, observations [10,13,14] indicate that turbulent slugs and spots most often originate in the entry region.

We show that exponential growth of disturbances in the entry region occurs at a Reynolds number of 1000, an order of magnitude lower than predicted by earlier theoretical work. Thus, linear instability can play a more important role on the route to turbulence than estimated up to now. We bring a recently developed sophisticated solution method for nonparallel stability to bear on this problem. This is the first time, to our knowledge, that this problem is solved in a consistent manner. Recent work on entry flow is either on finite amplitude perturbations [15,16] or on estimates of transient growth [17], not on linear instability. The existence of exponential growth, even over a short axial extent, means that transient growth and nonlinearities will be enhanced significantly, hastening the transition to turbulence.

A body of work on linear instability was done several decades ago, with large discrepancy among the theoretical results. For example, Tatsumi [18], Huang and Chen [19], Garg [20], and Gupta and Garg [21] obtained critical Reynolds numbers for linear instability, Re_{cr}, of 9700, 19,750, 13,250, and 11,700, respectively. The typical pipe is known to undergo a transition to turbulence at a far lower Reynolds number, of about 2000, in which case the linear instability in the entry region may be deemed to be of only academic interest. Probably due to this, the disagreements were never resolved. It is only recently that laminar flow has been achievable at Reynolds number exceeding 100,000, see, e.g., Ref. [2], in such cases the entry region will obviously play an important role in the transition to turbulence. The contrast with experiment, where linear instabilities were seen at a Reynolds number as low as 3800 [13], was not investigated. All theoretical studies of linear instability, to our knowledge, have made two major approximations: (i) the basic flow, whose stability is being studied, is taken in an approximate form, usually of boundary-layer type, and (ii) the stability is studied under the assumption of locally parallel flow. Both of these represent physics inadequately, as we find. Given the current interest in pipe transition, it is imperative to study this flow with better technique, which includes all the physics. As described in Sec. 2, we obtain the basic flow in a long entry region accurately. A nonparallel stability analysis is conducted, correct to $O(\mathrm{Re}^{-1})$ as described in Sec. 3.

2 Mean Flow

The flow studied here is through a straight pipe (shown in Fig. 1) with a uniform streamwise velocity U_i at the inlet. We solve the axisymmetric Navier–Stokes equations for steady, incompressible Newtonian flow in the stream function-vorticity formulation using a six-level full-multigrid method on a parallel machine. The equations are nondimensionalized by the streamwise velocity U_i at the inlet and the radius of the pipe R. The Reynolds number is thus $\mathrm{Re} \equiv U_i R/\nu$, where ν is the kinematic viscosity. A large enough length of pipe is considered for the Neumann condition to be applicable at the outlet, and the exit profile is checked to be parabolic. The details of the solution method and its validation are given in Refs. [22,23]. Axial (U) and radial (V) velocity profiles at different axial locations for Re=5000 are shown in Figs. 2(a) and 2(b), respectively. The exact solution is found to be considerably different from all the approximate profiles used in earlier studies.

3 Nonparallel Stability Analysis

3.1 Formulation. To study the stability of this flow, each quantity is expressed as the sum of a mean and a three-dimensional perturbation, e.g.,

$$u_{\mathrm{tot}} = U(x,r) + \hat{u}(x,r,\theta,t) \tag{1}$$

where x, r, and θ are the axial, radial, and azimuthal coordinates respectively; u, v and w are the corresponding velocity components; the subscript tot stands for "total;" and t is time. For $\mathrm{Re} \gg 1$, we have $\partial/\partial x \ll \partial/\partial r$, and therefore $V \sim O(\mathrm{Re}^{-1})$, as is verified numerically, see Fig. 2(b). This simplifies our approach, since it enables us to express the x dependence of the perturbations as the product of a rapidly varying wavelike part, $\exp[i\int \alpha(x)\mathrm{d}x]$, and a slowly varying function, $u(x,r)$, such that $\partial u/\partial x \sim O(\mathrm{Re}^{-1})$. The approach followed is thus similar to Ref. [22]. In combination with a normal mode form in θ and t, the streamwise velocity perturbation may be written as

Contributed by the Fluids Engineering Division of ASME for publication in the Journal of Fluids Engineering. Manuscript received November 10, 2006; final manuscript received May 22, 2007. Review conducted by Dimitris Drikakis.

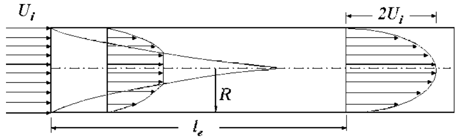

Fig. 1 Schematic of the developing flow in the entry region of a pipe; not to scale

$$\hat{u} = \mathrm{Re}\left\{ u(x,r)\exp\left[i\left(\int \alpha(x)\mathrm{d}x + n\theta - \beta t \right)\right]\right\} \tag{2}$$

where n is the number of waves in the azimuthal direction, and β is the disturbance frequency. The continuity and momentum equations are linearized, and terms of $O(\mathrm{Re}^{-2})$ and smaller terms are neglected. The final equation is of the form

$$\mathcal{H}\phi(x,r) + \mathcal{G}\frac{\partial \phi(x,r)}{\partial x} = \beta \mathcal{B}\phi(x,r) \tag{3}$$

Here $\phi=[u,v,w,p]^T$, and the nonzero elements of the 4×4 matrix operators $\mathcal{H}$, $\mathcal{G}$, and $\mathcal{B}$ are given by

$$h_{11} = Ui\alpha + \mathcal{D}_x U + V\mathcal{D}_r + \mathcal{Q} - \frac{1}{\mathrm{Re}}\frac{1}{r^2} \quad h_{12} = \mathcal{D}_y U$$

$$h_{14} = i\alpha \quad h_{23} = \frac{2}{\mathrm{Re}}\frac{in}{r^2} \quad h_{22} = V\mathcal{D}_r + \mathcal{D}_r V + Ui\alpha + \mathcal{Q}$$

$$h_{24} = \mathcal{D}_r \quad h_{32} = -\frac{2}{\mathrm{Re}}\frac{in}{r^2} \quad h_{33} = V\mathcal{D}_r - \frac{V}{r} + Ui\alpha + \mathcal{Q}$$

$$h_{34} = \frac{in}{r} \quad h_{41} = \frac{i\alpha}{\mathrm{Re}}\mathcal{D}_r \quad h_{42} = V\mathcal{D}_r + \mathcal{D}_r V + Ui\alpha$$

$$+ \frac{1}{\mathrm{Re}}\left(\frac{n^2}{r^2} + \alpha^2\right) \quad h_{43} = \frac{in}{\mathrm{Re}}\left(\frac{1}{r^2} + \frac{\mathcal{D}_r}{r}\right) \quad h_{44} = \mathcal{D}_r$$

$$g_{11} = g_{22} = g_{33} = g_{42} = U \quad g_{14} = 1$$

and

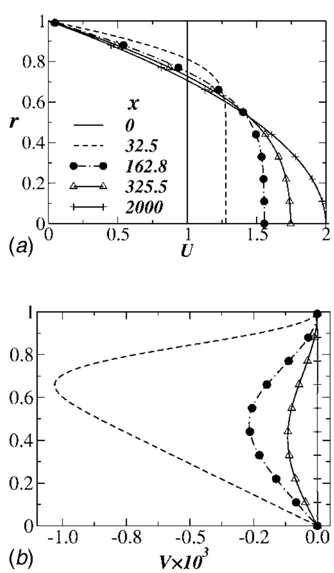

Fig. 2 (*a*) Axial and (*b*) radial velocity profiles at different streamwise locations; Re=5000

$$b_{11} = b_{22} = b_{33} = b_{42} = i \quad \text{where } \mathcal{D}_r = \frac{\partial}{\partial r}$$

$$\mathcal{D}_x = \frac{\partial}{\partial x}$$

and

$$\mathcal{Q} = \frac{1}{\mathrm{Re}}\left[\alpha^2 + \frac{(1+n^2)}{r^2} - \frac{1}{r}\frac{\partial}{\partial r} - \frac{\partial^2}{\partial r^2}\right]$$

The boundary conditions are

$$u = v = w = p = 0 \quad \text{at } r=0 \quad \text{for } n \neq 1 \tag{4}$$

$$u = p = 0 \quad v + iw = 0 \quad \text{at } r=0 \quad \text{for } n=1 \tag{5}$$

$$u = v = w = 0 \quad \text{at } r=1 \tag{6}$$

Incidentally, Eq. (3) may be obtained from the stability equation in Ref. [22] by setting the angle of pipe divergence to zero. The system of partial differential equations obtained here may be solved as an eigenvalue problem of larger size as described in the following section.

3.2 Solution Method. The streamwise derivative in Eq. (3) couples neighboring axial locations in the flow field to one another. Consider two streamwise Locations 1 and 2 separated by an incremental distance, i.e., $x_2=x_1+\Delta x$. To first order in Δx, and noting that β remains constant downstream, we may express Eq. (3) as

$$\begin{bmatrix} \mathcal{H}_1 - \mathcal{G}_1/\Delta x & \mathcal{G}_1/\Delta x \\ -\mathcal{G}_2/\Delta x & \mathcal{H}_2 + \mathcal{G}_2/\Delta x \end{bmatrix}\begin{bmatrix}\phi_1 \\ \phi_2\end{bmatrix} = \beta \begin{bmatrix}\mathcal{B}_1 & 0 \\ 0 & \mathcal{B}_2\end{bmatrix}\begin{bmatrix}\phi_1 \\ \phi_2\end{bmatrix} \tag{7}$$

The partial differential equation now has the appearance of an eigenvalue problem of twice the size of the corresponding parallel stability problem. The discretization and solution of the eigensystem are done using a Chebyshev collocation spectral method, described, for example, in Ref. [24]. The collocation points given by

$$y_i = \cos(i\pi/N) \quad i = 1,N \tag{8}$$

are naturally denser near the wall and sparser close to the centerline, so no further grid stretching is necessary. The results shown here have been obtained with 81 grid points; the accuracy is discussed later in this section.

Note that in Eq. (2), the x dependence may be apportioned arbitrarily between α and the eigenfunction u as long as all rapid variations in the axial direction are included in the wavelike part, to ensure that $\partial u/\partial x$ is small. To do this, we first set the operator $\mathcal{G}$ to zero and solve the resulting eigenvalue problem at Locations 1 and 2 independently. At each location, we choose a guess value of α and iterate it until the desired complex frequency β_0 is obtained. The operators $\mathcal{H}$, $\mathcal{G}$, and $\mathcal{B}$ are then known at Locations 1 and 2, so Eq. (7) can be solved. This procedure works since the ordinary differential equation differs from the partial differential equation only in terms nominally of $O(\mathrm{Re}^{-1})$. We have verified numerically that choosing other suitable initial guesses for $\mathcal{G}$ makes no difference to the results.

The growth rate g of the disturbance kinetic energy, $E=1/2(\hat{u}^2+\hat{v}^2+\hat{w}^2)$, is given by

$$g = \frac{1}{E}\frac{\partial E}{\partial x} = -2\alpha_i + \left.\frac{1}{E_e}\frac{\partial E_e}{\partial x}\right|_r \tag{9}$$

where $E_e=1/4(uu^*+vv^*+ww^*)$, the asterisk denotes a complex conjugate. It is characteristic of developing flow that a disturbance may amplify at one radial location and decay at another. Secondly, one disturbance quantity (e.g., $\hat{u}$) could be amplified while others decay.

Typical values of α obtained by using different numbers of

Table 1 Sensitivity of wavenumber and growth rate to the number of collocation points used

No. of grid points (N)	α_r	α_i
51	0.499990	−0.000748914
61	0.490003	−0.000744894
81	0.490001	−0.000743789

collocation points for Re=5000, $x=183.5$, and $\beta_d=0.5$ are shown in Table 1. It is seen that 81 grid points are sufficient to make a statement about stability.

4 Results and Discussion

Present eigenvalues for fully developed pipe flow match with those of Ref. [25] up to the tenth decimal place. While the least stable mode for fully developed flow is the helical ($n=1$) mode, the axisymmetric ($n=0$) mode is found to be the most unstable here, consistent with experiment [13]. At Re=5000, the variation with axial distance of amplitude of disturbance kinetic energy is shown in Fig. 3. Disturbances of frequencies outside the range shown are found to be less unstable. The variation is monitored here at $r=0.08$. The flow is linearly unstable within a certain axial extent. Too far upstream, the effective Reynolds number of the shear layer is too low for instability, and downstream; the flow is closer to fully developed and thus linearly stable. It is found (not shown) that the disturbance kinetic energy decays for $r>0.6$, and that its growth is maximum close to the centerline. Thus an experiment where the probe is positioned within $0<r<0.6$ would measure exponential growth of disturbances of the right frequency, while probes placed closer to the wall would register a stable flow. The disturbance kinetic energy integrated across the pipe decays at these Reynolds numbers. We thus expect a greater tendency toward turbulence close to the centerline, in contrast with other mechanisms.

Under the parallel flow approximation, earlier studies neglected the "small" variations in the downstream direction, as well as the small radial mean flow. With consistent matched asymptotic expansions in the distinguished limits, it has been shown that these effects are not small [26]. In fact, the axial development of the flow makes $O(1)$ contributions over some radial extent. The largest effects come from the terms in the stability equations containing V multiplied by a radial derivative of the eigenfunction, as we found numerically and from the estimates of order of magnitude. What is happening physically is that the negative radial mean flow sweeps disturbance vorticity away from the wall and toward the centerline, which affects stability dramatically. The parallel flow approximation, even using the accurate basic flow, completely misses this physics and finds the flow to be stable, as seen in Fig. 3.

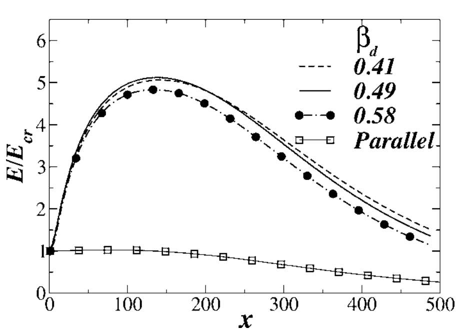

Fig. 3 Amplification of the disturbance kinetic energy for the axisymmetric ($n=0$) mode for typical disturbance frequencies for Re=5000 at $r=0.08$. The result with a parallel flow assumption is shown by the solid line with squares.

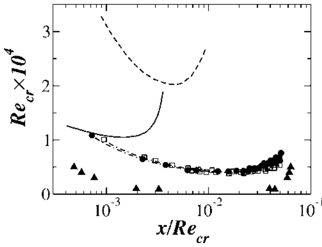

Fig. 4 Axial variation of the critical Reynolds number. Filled triangles, axisymmetric mode at $r=0.25$. Filled circles and open squares, experimental results [13]. The theoretical results of Refs. [18,19] for axisymmetric disturbances are shown by the dashed and solid lines, respectively. The results of Refs. [13,18,19] were compliled in this manner in Ref. [15].

In the experiments compiled by [13], the variation in amplitude of the axial disturbance velocity $\hat{u}$ was the quantity measured, which gives the result integrated over all eigenmodes. Since only a small range of frequencies is unstable at the Reynolds numbers considered, we expect the experiment to display a significantly lower level of instability than predicted by the stability analysis. We also do not expect $\hat{u}$ to correlate exactly with E. Also, stability is a function of r, and the measurements were made at one or more unspecified radial locations. Figure 4 shows the present zero growth curve at $r=0.25$. The region above the curves is unstable, indicating the axial extent of possible exponential growth at a given Reynolds number. The qualitative behavior is the same as the experiments, with a larger region of instability, as expected. Note that at a Reynolds number of 1000, the flow is already linearly unstable over a short axial extent. The growth rates (not shown) at this Reynolds number, however, are extremely small and would be difficult to see in an experiment. The effect of these modes on the transition at this Reynolds number would be indirect, via transient growth, but probably already not insignificant. It is clear from the same figure that the critical Reynolds numbers predicted by earlier theoretical studies are unrealistically high. Figure 5(a) demonstrates that at $r=0.25$, while the predicted neutral boundary is larger than in the experiments, the extent over which the kinetic energy grows by 1.8 times or more of its original amplitude matches very well with the experimental neutral boundary. A modern experiment where instability of a given frequency could be detected accurately at a specified radial location would be very valuable. The regions of instability at different radial locations are shown in Fig. 5(b). In accordance with the expectations above, disturbance growth is much higher closer to the centerline rather than at the wall. In the existing experiments, the radial location at which measurements were made is not mentioned; the prediction here that disturbance growth is a sensitive function of the radial location will hopefully motivate further experimental work.

To summarize, flow in the entry region of a pipe is already linearly unstable at a Reynolds number of 1000, an order of magnitude lower than computed hitherto, so this region could play a more important role in transiiton to turbulence than realized. The advection toward the centerline of the disturbance vorticity by the small radial mean flow is the generator of this instability. We have made no approximation in solving for the mean flow and have performed a complete nonparallel analysis correct to $O(\mathrm{Re}^{-1})$. Our results are in qualitative agreement with existing experiment, but more accurate experiments are needed. The present instability is axisymmetric and most active near the centerline, which clearly distinguishes it from other mechanisms of transition to turbulence, such as low-speed streaks. This would make it more appealing to the experimenter.

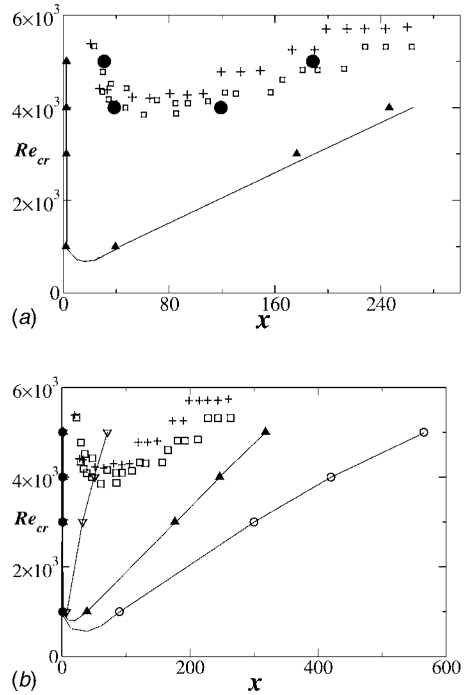

Fig. 5 Axial variation of the critical Reynolds number ($n=0$ mode). Plus and open squares: experimental results [13] for nonaxisymmetric and axisymmetric disturbances, respectively. (*a*) At $r=0.25$. Filled triangles, neutral boundary; filled circles, where $E/E_{cr}=1.8$. (*b*) Open circles, $r=0.5$; filled triangles, $r=0.25$; open triangles, $r=0.08$. The lines are shown to guide the eye.

Acknowledgment

Grateful thanks to Professor Tom Mullin for the thesis of S. D. Williams and for discussions. We acknowledge the Defense Research and Development Organisation, India for financial support.

References

[1] Lessen, M., Sadler, S. G., and Liu, T. Y., 1968, "Stability of Pipe Poiseuille Flow," Phys. Fluids, **11**, pp. 1404–1409.

[2] Hof, B., van Doorne, C. W. H., Westerweel, J., Nieuwstadt, F. T. M., Faisst, H., Eckhardt, B., Wedin, H., Kerswell, R. R., and Waleffe, F., 2004, "Experimental Observation of Nonlinear Traveling Waves in Turbulent Pipe Flow," Science, **305**, pp. 1594–1598.

[3] Hof, B., Juel, A., and Mullin, T., 2003, "Scaling of the Turbulence Transition Threshold in a Pipe," Phys. Rev. Lett., **91**, pp. 244502.

[4] Peixinho, J., and Mullin, T., 2006, "Decay of Turbulence in Pipe Flow," Phys. Rev. Lett., **96**, pp. 094501.

[5] Kerswell, R. R., 2005, "Recent Progress in Understanding the Transition to Turbulence in a Pipe," Nonlinearity, **18**, pp. R17–R44.

[6] Faisst, H., and Eckhardt, B., 2006, "Traveling Waves in Pipes," Phys. Rev. Lett., **91**, pp. 224502.

[7] Hof, B., van Doorne, C. W. H., Westerweel, J., and Nieuwstadt, F. T. M., 2005, "Turbulence Regeneration in Pipe Flow at Moderate Reynolds Numbers," Phys. Rev. Lett., **95**, pp. 214502.

[8] Waleffe, F., 1998, "Three-Dimensional Coherent States in Plane Shear Flows," Phys. Rev. Lett., **81**(19), pp. 4140–4143.

[9] Ekman, V. W., 1910, "On the Change From Laminar to Turbulent Motion of Liquids," Ark. Mat., Astron. Fys., **6**, pp. 1–16.

[10] Wygnanski, I. J., and Champagne, F. H., 1973, "On Transition in a Pipe. Part 1. The Origin of Puffs and Slugs and the Flow in a Turbulent Slug," J. Fluid Mech., **59**, pp. 281–335.

[11] Reshotko, E., 1958, "Experimental Study of the Stability of Pipe Flow I. Establishment of an Axiallary Symmetric Poiseuille Flow," *JPL Progress Report* No. 20-364.

[12] Huerre, P., and Rossi, M., 1998, *Hydrodynamics and Nonlinear Instabilities*, C. Godreche and P. Manneville, eds., Cambridge University Press, Cambridge, p. 81.

[13] Sarpkaya, T., 1975, "A Note on the Stability of Developing Laminar Pipe Flow Subjected to Axisymmetric and Non-axisymmetric Disturbances," J. Fluid Mech., **68**, pp. 345–351.

[14] Sarpkaya, T., 1966, "Experimental Determination of the Critical Reynolds Number for Pulsating Poiseuille Flow," ASME J. Basic Eng., **88**, pp. 589–598.

[15] Williams, S. D., 2001, "An Investigation of the Stability of Developing Pipe Flow," Ph.D. thesis, University of Manchester, Manchester, UK.

[16] Moss, E. A., and Abbot, A. H., 2002, "The Effect of Finite Amplitude Disturbance Magnitude on Departures from Laminar Conditions in Impulsively Started and Steady Pipe Entrance Flows," ASME J. Fluids Eng., **124**(1), pp. 236–240.

[17] Duck, P. W., 2005, "Transient Growth in Developing Plane and Hagen Poiseuille Flow," Proc. R. Soc. London, Ser. A, **461**, pp. 1311–1333.

[18] Tatsumi, T., 1952, "Stability of the Laminar Inlet-flow Prior to the Formation of Poiseuille Regime. II," J. Phys. Soc. Jpn., **7**, pp. 495–502.

[19] Huang, L. M., and Chen, T. S., 1974, "Stability of the Developing Laminar Pipe Flow," Phys. Fluids, **17**(1), pp. 245–247.

[20] Garg, V. K., 1981, "Stability of Developing Flow in a Pipe Flow: Non-axisymmetric Disturbances," J. Fluid Mech., **110**, pp. 209–216.

[21] Gupta, S. C., and Garg, V. K., 1981, "Effect of Velocity Distribution on the Stability of Developing Flow in a Pipe," Phys. Fluids, **24**(4), pp. 576–578.

[22] Sahu, K. C., and Govindarajan, R., 2005, "Stability of Flow Through a Slowly Diverging Pipe," J. Fluid Mech., **531**, pp. 325–334.

[23] Sahu, K. C., 2003, Master's thesis, Jawaharlal Nehru Centre for Advanced Scientific Research, Bangalore, India.

[24] Canuto, C., Hussaini, M. Y., Quarteroni, A., and Zang, T. A., 1987, *Spectral Methods in Fluid Dynamics*, Springer-Verlag, New York.

[25] Schmid, P. J., and Henningson, D. S., 2001, *Stability and Transition in Shear Flows*, Springer-Verlag, New York.

[26] Govindarajan, R., and Narasimha, R., 1999, "A Low-order Parabolic Theory for Two-dimensional Boundary Layer Stability," Phys. Fluids, **11**(6), pp. 1449–1458; Bhattacharya, P., Manoharan, M. P., Govindarajan, R., and Narasimha, R., 2006, "The Critical Reynolds Number of a Laminar Incompressible Mixing Layer from Minimal Composite Theory," J. Fluid Mech., **565**, pp. 105–114.